Cytotoxicity Assessment of Surface-Modified Magnesium Hydroxide Nanoparticles

Echeverry-Rendon, Monica; Stancic, Brina; Muizer, Kirsten; Duque, Valentina; Calderon, Deanne Jennei; Echeverria, Felix; Harmsen, Martin C.

Published in:
ACS Omega

DOI:
10.1021/acsomega.1c06515

Publication date:
2022

ACS OMEGA

http://pubs.acs.org/journal/acsodf

Article

Cytotoxicity Assessment of Surface-Modified Magnesium Hydroxide Nanoparticles

Mónica Echeverry-Rendón,* Brina Stančič, Kirsten Muizer, Valentina Duque, Deanne Jennei Calderon, Felix Echeverria, and Martin C. Harmsen*

Cite This: *ACS Omega* 2022, 7, 17528−17537

Read Online

ACCESS | Metrics & More | Article Recommendations | Supporting Information

ABSTRACT: Magnesium-based nanoparticles have shown promise in regenerative therapies in orthopedics and the cardiovascular system. Here, we set out to assess the influence of differently functionalized Mg nanoparticles on the cellular players of wound healing, the first step in the process of tissue regeneration. First, we thoroughly addressed the physicochemical characteristics of magnesium hydroxide nanoparticles, which exhibited low colloidal stability and strong aggregation in cell culture media. To address this matter, magnesium hydroxide nanoparticles underwent surface functionalization by 3-aminopropyltriethoxysilane (APTES), resulting in excellent dispersible properties in ethanol and improved colloidal stability in physiological media. The latter was determined as a concentration- and time-dependent phenomenon. There were no significant effects on THP-1 macrophage viability up to 1.500 μg/mL APTES-coated magnesium hydroxide nanoparticles. Accordingly, increased media pH and Mg^{2+} concentration, the nanoparticles dissociation products, had no adverse effects on their viability and morphology. HDF, ASCs, and PK84 exhibited the highest, and HUVECs, HPMECs, and THP-1 cells the lowest resistance toward nanoparticle toxic effects. In conclusion, the indicated high magnesium hydroxide nanoparticles biocompatibility suggests them a potential drug delivery vehicle for treating diseases like fibrosis or cancer. If delivered in a targeted manner, cytotoxic nanoparticles could be considered a potential localized and specific prevention strategy for treating highly prevalent diseases like fibrosis or cancer. Looking toward the possible clinical applications, accurate interpretation of in vitro cellular responses is the keystone for the relevant prediction of subsequent in vivo biological effects.

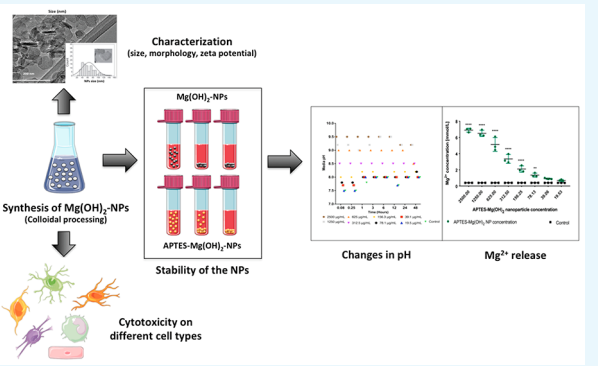

1. INTRODUCTION

In the development of novel medical therapeutic modalities, nanotechnology is receiving considerable attention. By their versatile composition and nature, nanoparticles (NPs) are increasingly recognized for their biomedical applications, such as drug and gene delivery vehicles, antibacterial agents, molecular diagnostics, tissue engineering, and cancer therapy.[1] Because of their unique mechanical, physicochemical, and tunable properties, NPs promise improved efficacy of established therapeutics, surpassing difficulties in crossing biological barriers,[2] increasing concentrations at the target location, and minimizing unwanted side effects.[3] Interaction of particles toward divalent cation-based NPs, cell internationalization, and material chemistry determine its potential and utility for a specific application. On the other side, functionalization, namely, adding active biomolecules or fluorophores to track the particles in the system, is of special interest, as it permits more localized treatments. Current progress in medicine is focused on treating diseases in a low invasive and personalized way. In medicine, the NPs are often used for drug delivery to change the cell environment, to promote cell repair; or oppositely, to kill and attack defective cells or tissue. One example of the latter application is cancer treatment, where chemotherapy, the current therapeutic option, is highly toxic, compromising the general health condition of the patients and impacting the overall costs. Despite the numerous promising aspects regarding the use of NPs, morphological changes, oxidative stress, and DNA damage[4,5] can have hazardous side effects upon NP administration, which may limit their medical use, thus raising concerns about their clinical safety.[2] However, if successfully targeted toward diseased cells, the unfavorable toxic characteristics can be exploited as beneficial traits, thus bringing new hopes for developing targeted disease therapy.

Received: November 19, 2021
Accepted: March 23, 2022
Published: May 19, 2022

Because of the specific features of cells and tissues, the toxicity and biological effect of NPs can differ between them. Materials with different compositions and properties, such as size and chemistry, have been explored. Some of the most used metal materials include gold, silver, copper, iron, zinc, and titanium oxide. Compared with those materials, magnesium (Mg) particles have been less explored despite their interesting properties. As a benefit, Mg is an essential element for the body, which plays an important role in processes involved in nerve function, regulating blood sugar levels and blood pressure, controlling the muscle and bone, and processing DNA and proteins. Mg also acts as a cofactor in more than 300 enzyme systems. Mg and, more specifically, MgOH or MgO are easily hydrolyzable and well-tolerated by the body. Previous studies have shown that Mg-NPs pose antibacterial properties by disrupting the bacterial membrane generating of reactive oxygen species (ROS).[6−9] Other biological applications of Mg-NPs include their ability to increase bone regeneration by enhancing cell adhesion and proliferation of osteoblasts and to cause relief of cardiovascular diseases, such as heartburn.[1,7,10−12]

Additionally, their potential for the eliminating cancer cells and their toxicity toward multiple cells and tissue types, such as liver, lung, and even bone marrow, have also been recognized.[1,5,7,13−19] Despite all these beneficiary properties, Mg is a highly reactive material that induces changes in the biological environment by modification of pH and by the gas hydrogen release. As mentioned before, Mg particles can be used as vehicle particles if the degradation stability is controlled or oppositely, as a killer agent to destroy a specific cellular group. One of the biggest challenges regarding the NPs used in medical applications is related to the physiological accumulation of these particles in the system, their distribution, storage, and possible damage in the short and long-term. However, as Mg is a degradable material, this effect can be less critical than in the case of other metals.[20,21] Considering the efforts taken until now, the toxicity of Mg-based NPs toward the cellular mediators of different diseases remains an area of potential interest. Because of its simple, cost-effective, and straightforward fabrication method,[13] as well as its exhibited aptitude for surface functionalization, magnesium hydroxide ($Mg(OH)_2$) was selected to be studied as a candidate material for biomedical applications. Improved knowledge of this material may explore its use as a drug delivery system rather than a toxic agent aimed to eradicate diseases such as cancer or fibrosis. In this context, this study aimed to investigate the effect of magnesium hydroxide NPs ($Mg(OH)_2$-NPs) toward different cell types and its optimization for being used in biomedical applications.

2. RESULTS

2.1. Morphology and Size Distribution of the $Mg(OH)_2$-NPs. The morphology of the $Mg(OH)_2$-NPs was confirmed by TEM, demonstrating that NPs consisted of irregular hexagonal platelets with their edges parallel, an average size of 65.1 ± 26 nm, with a max/min length over the axes between 28 and 147 nm and a thickness of 11.54 ± 2.11 nm (Figure 1).[22] According to the nanosight analysis, the mean size of the particles was 89.0 ± 17 nm; however, the limitation of this technique is that particles are interpreted as roundish spheres. Additionally, four size populations (peaked at 35, 95, 155, and 215 nm average size) are discerned from nanoparticle tracking analysis. These varieties can be related to aggregates.

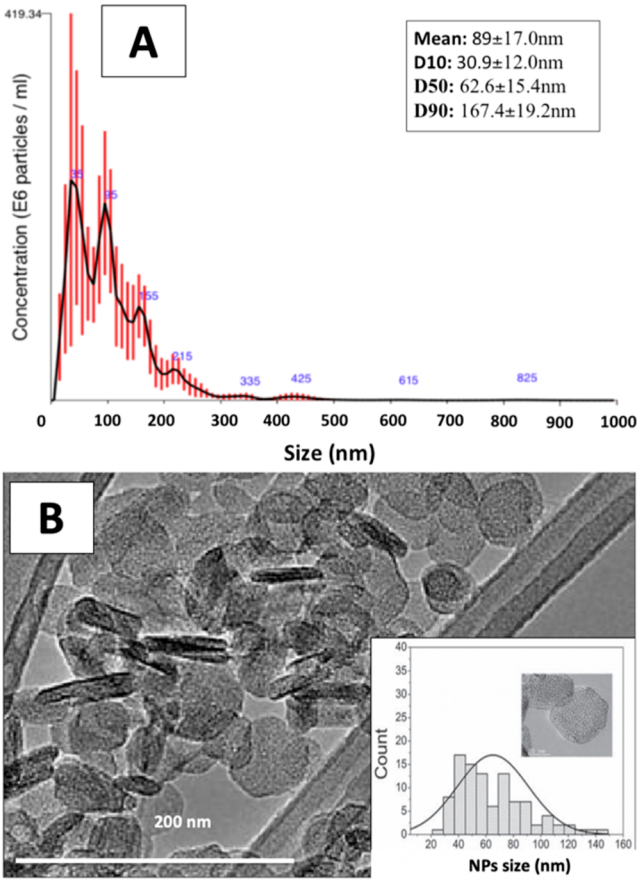

Figure 1. $Mg(OH)_2$-NPs generated by precipitation are shaped as hexagonal platelets. (A) NTA-determined size distribution of $Mg(OH)_2$-NPs and (B) TEM images of $Mg(OH)_2$ hexagonal NPs.

2.2. Toxicity of the $Mg(OH)_2$-NPs. Results from MTT are shown in Figure 2. The cytotoxicity was calculated based on the measurement of the mitochondrial activity of the cells once they were exposed to different concentrations of bare NPs and normalizing the values obtained to the control of which were untreated cells. According to the standard ISO 10993 (for medical device biocompatibility testing), a compound or material is considered toxic for percentages less than 70% of, in this case, mitochondrial activity. Bare NPs at the lowest concentration were noncytotoxic to mesenchymal cells (ASC, HDF, PK84), with a mitochondrial activity in the range of 85−100%, while monocytic cells and ECs were far less resilient, showing a 50% to 70% of regular mitochondrial activity already at the lowest NP concentration (Figure 2). According to this, cells, such as HUVECs, HPMECs, and THP-1 cells, have increased sensitivity to nanomaterials medium, while oppositely, HDF, ASCs, and PK84 are more resistant to the effect of Mg.

Precipitation of aggregated NPs was an inevitable concentration-dependent phenomenon when the latter increased to 2.500 μg/mL. Additionally, this explained the formation of the NP crust that suffocated the cells at 2.500 μg/mL in the cytotoxicity assays. Nevertheless, precipitation was only observed in the first three serial dilutions, namely, 2.500, 1.250, and 625 μg/mL, being monitored for 48 h, with a clear suspension observed from 312.5 μg/mL downward.

https://doi.org/10.1021/acsomega.1c06515
ACS Omega 2022, 7, 17528−17537

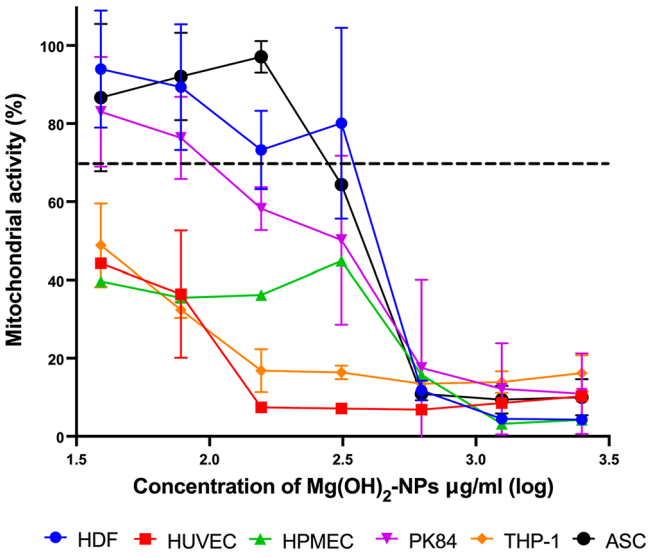

Figure 2. Cytotoxicity effect of $Mg(OH)_2$-NPs suspensions (2.500−19.5 μg/mL) for 48 h in different cell lines HDF, HUVEC, HPMEC, PK84, THP-1, and ASCs. According to the ISO 10993-5 standard values <70% are considered toxic.

Because of they had the best results in terms of biocompatibility, ASCs and PK84 cells were selected for cell configuration studies. Cytoskeleton staining was performed to determine the morphological changes. The staining showed that, with increasing $Mg(OH)_2$-NPs concentration, the number of cells decreases and the morphology of the cells changes; namely, they become smaller and start to fall apart (Figures S1 and S2).

Because of the importance of macrophages and their interaction with NPs in the immune system, THP-1 cells were selected to continue the studies regarding the stability and effects of biological $Mg(OH)_2$-NPs. Additionally, THP-1 cells were part of the group that showed more susceptibility to $Mg(OH)_2$-NPs, a reason an improvement in the biocompatibility of the NPs was needed.

2.3. Zeta Potential. The measurements of the zeta potential of both the NPs without functionalization and those functionalized were 36.8 ± 2.2 and 39.2 ± 1.4 mV, respectively. It is well-known that for zeta potentials above ±30 mV, it is expected to a good stability of the NPs in solution.

2.4. Dispersion and Toxicity of APTES-$Mg(OH)_2$-NPs. Initial experiments revealed high instability, low dispersible properties, and increased sedimentation rates at higher concentrations. Aggregates with a size of several micrometers had uniformly precipitated to the bottom and could not be removed nor dissipated by extended direct ultrasonication. Consequently, these particle aggregates may have formed a cytotoxic crust, increasing the cytotoxicity effect. This warranted functionalization of the NPs using organosilane coupling agents.

Visual monitoring of APTES-$Mg(OH)_2$-NP's colloidal stability revealed good dispersible properties in EtOH, while NP stability was different when introduced into an aqueous system. A precipitate could be observed after 24 h of incubation in dH_2O, while in EtOH, a suspension was maintained during the 48 h (Figure S3-A). Improved dispersibility of amino-silanized NPs in cell culture media was observed after 1 h, at which the uncoated particles were already completely aggregated (Figure S3-B). However, after 24 h, again, a precipitate of aggregated NPs had formed (Figure S3-B). It was postulated that the aminosilane affinity for −OH group of polar solvents (dH_2O, EtOH), in which the silanization reaction was carried out, could have resulted in incomplete functionalization of $Mg(OH)_2$-NPs, and instead, formation of silicate NPs. To that end, the protocol was optimized by using dimethylformamide (DMF) as an apolar organic solvent, which provided more favorable conditions that resulted in improved colloidal stability in aqueous solution of APTES-$Mg(OH)_2$-NPs for up to 24 h (Figure S3-C), confirming a serum-concentration dependent effect.

When the culture medium was used, the presence of FBS improved the dispersion of the particles, which the increased viscosity of the solution could explain. The dispersible properties and precipitation rates were further evaluated by mimicking different cell culture conditions. Larger aggregates and thus faster sedimentation were observed upon incubation with serum-free cell culture medium, compared to culture medium with 3% or 10% FBS, respectively. Therefore, a medium with 10% FBS was selected as the cell culturing condition for the following assays since protein (FBS) prevented aggregation of functionalized particles (but not of bare NPs) (Figure S3-C).

Considering the now improved dispersible properties of functionalized APTES-$Mg(OH)_2$-NPs, we next aimed to test their cytotoxicity compared to their bare counterpart. To simplify the experimental setup and to evaluate whether functionalization improves improving cytotoxic properties, a highly sensible cell line was required. For this reason, THP-1 macrophages were selected for further experiments. Additionally, they were selected because of their role in phagocytosis and foreign body response. As shown in Figure 3, APTES-

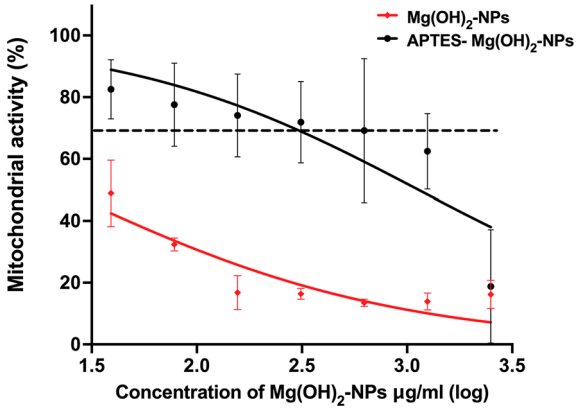

Figure 3. Mitochondrial activity of THP-1 cells exposed to $Mg(OH)_2$-NPs with and APTES functionalization. According to the ISO 10993-5 standard values <70% are considered toxic.

$Mg(OH)_2$-NPs exhibited low cytotoxic properties in THP-1 macrophages, with substantially decreased viability only observed at 2.500 μg/mL. Compared to bare $Mg(OH)_2$-NPs, the THP-1 viability almost doubled, confirming that aggregates strongly contributed to cytotoxic properties of bare $Mg(OH)_2$-NPs. Therefore, it was concluded that, unless exposed to extremely high concentrations, APTES-$Mg(OH)_2$-NPs were cytocompatible with THP-1 macrophages.

Despite the low dissolution properties of $Mg(OH)_2$-NPs, their release of Mg^{2+} ions and hydroxide anions (OH^-) could represent a possible toxicity-inducing mechanism. The NP

https://doi.org/10.1021/acsomega.1c06515
ACS Omega 2022, 7, 17528−17537

effect on the media pH was monitored in a concentration range of 2,500 to 19.5 μg/mL during 48 h incubation in acellular conditions. Upon introducing the cell culture media, there was an immediate increase of OH^- ions; hence, the media pH, was observed with limited alteration throughout 48 h (Figure 4). Moreover, the exposure to NP concentrations of

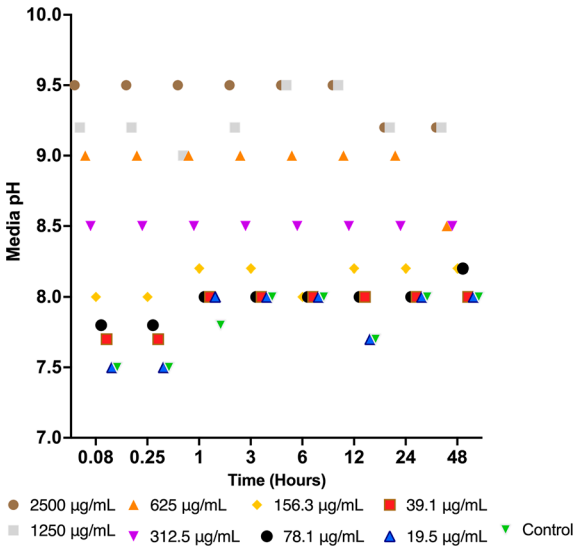

Figure 4. APTES-$Mg(OH)_2$-NPs in acellular conditions (culture medium) and incubated at 37 °C for 5 min, 15 min, 1 h, 3 h, 6 h, 12 h, 24 h, and 48 h, respectively. The pH measured at all the time points showed a significant increase upon exposure to 2500, 1250, 625, 312.5, 156.3, 78.1, 39.1, and 19.5 μg/mL compared to the control media.

2500, 1250, 625, and 312.5 μg/mL, respectively, resulted in a significant pH increase compared to the control media. Furthermore, the influence was shown to be concentration-dependent, with the highest alkalinity (9.5) reached at 2500 μg/mL.

Corresponding to the time-dependent OH^- release, hence pH media change; similar trends were observed in Mg^{2+} concentration monitored at 300 μg/mL NPs concentration for 48 h (Figure 5A). Moreover, the dissolution kinetics analysis, with 45.7% (5 min) to 56.8% (24 h) dissolved APTES-$Mg(OH)_2$-NPs (Figure 5B), indicated NP dissolution potential to be reached almost instantly, hence confirming high NP reactivity and rapid NP dissolution upon the introduction of physiological media.

NP concentration-dependent effect on media pH was further reflected in the Mg^{2+} release monitored during 48 h incubation, where significantly increased Mg^{2+} levels detected at the concentration range of 2500 to 78.13 μg/mL proved that NPs dissolve in a concentration-dependent manner (Figure 6A). However, highly increased Mg^{2+} levels observed at high nanoparticle concentrations were attributed only to a small proportion of dissolved nanoparticles (15.2% at 2500 μg/mL), while low Mg^{2+} levels measured at low nanoparticle concentrations were a result of almost complete nanoparticle dissolution (89.6% at 19.5 μg/mL) (Figure 6B).

Given the strong media alkalinity and Mg^{2+} release at high NPs concentrations, the contribution of these factors to the exhibited NPs cytotoxicity was investigated. The specific effects of the alkaline supernatant collected after 48 h NP incubation (pH 9.5−7.5 with concerning NP concentration

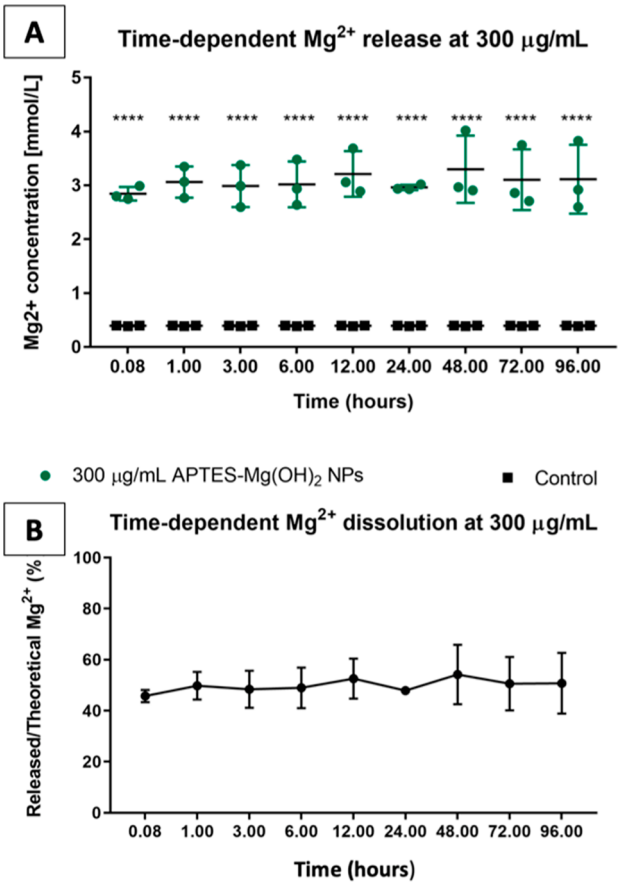

Figure 5. Dissolution potential of APTES- $Mg(OH)_2$-NPs is reached almost immediately. APTES-$Mg(OH)_2$-NPs in acellular conditions (culture medium), incubated at 37 °C for 5 min, 1 h, 3 h, 6 h, 12 h, 24 h, and 48 h, respectively. The Mg^{2+} concentration showed a significant increase at all the time points compared to the control media (A) and only limited changes over time (B). (****$p < 0.0001$).

2500−19.5 μg/mL) on THP-1 macrophage morphology were evaluated by comparison toward pH-adjusted neutral media with respective Mg^{2+} concentrations. Compared to the control medium (Figure S4D), THP-1 cells cultured in alkaline media (Figure S4A−C) had normal undifferentiated morphology. No morphological changes were observed in the supernatants corresponding to NP concentration range of 2500−19.5 μg/mL (Figure S4E−G), in which the pH was adjusted to neutral, and after its comparison with the control (Figure S4H).

The results of the morphological analysis were further substantiated by subjecting the same conditions to an MTT assay, where Mg^{2+} ions and alkaline pH media of respective NP-incubated supernatants exhibited no cytotoxic effects toward THP-1 macrophages (Figure 7). Alternatively, supernatant with high Mg^{2+} concentration and alkaline pH media exhibited favorable effects compared to the equivalent condition with neutral media pH.

Lastly, the effect of released Mg^{2+} in cell culture media supernatants of 48h-incubated APTES-$Mg(OH)_2$-NPs was confirmed by extrapolating THP-1 macrophage viability from $MgCl_2$ standard curve. The $MgCl_2$ standard curve indicated 50 mmol/L Mg^{2+} as the IC_{50} concentration for THP-1 macrophages. Alternatively, measured Mg^{2+} release concerning NPs concentration range of 2500−19.5 μg/mL indicated much lower Mg^{2+} concentrations (6.50−0.30 mM, respectively);

https://doi.org/10.1021/acsomega.1c06515
ACS Omega 2022, 7, 17528−17537

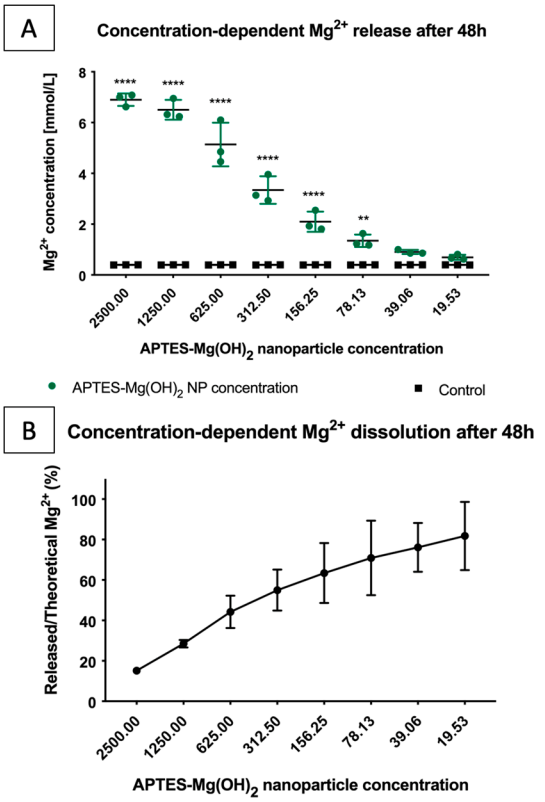

Figure 6. Concentration-dependent NPs dissolution potential reflects in concentration-dependent Mg^{2+} release. APTES-$Mg(OH)_2$-NPs (2500−19.5 μg/mL) in acellular conditions (culture medium), incubated at 37 °C for 48 h. The Mg^{2+} concentration showed a significant increase compared to the control media (A) and the range of nanoparticle dissolution potential (B) (****$p < 0.0001$).

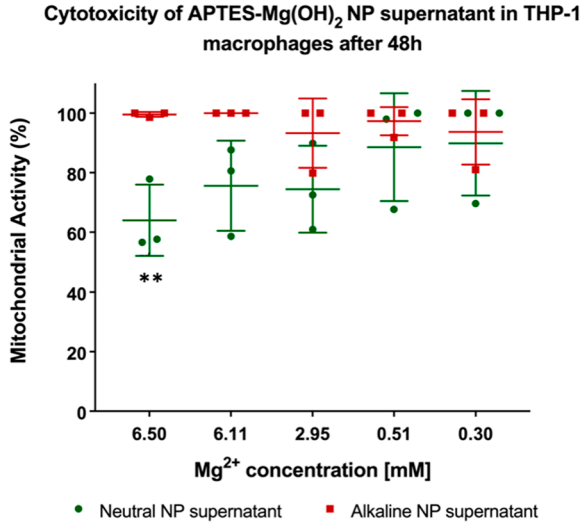

Figure 7. Alkaline pH and Mg^{2+} concentration in supernatant corresponding to 2500−19.5 μg/mL NPs concentration range do not exhibit cytotoxic effects in THP-1 macrophages. APTES-$Mg(OH)_2$-NPs (2500−19.5 μg/mL) were resuspended in acellular conditions (culture medium) for 48 h at 37 °C. After centrifugation, THP-1 macrophages were exposed to respective supernatants for 48 h at 37 °C. Increased Mg^{2+} levels showed no toxic effects, while alkaline pH affected THP-1 mitochondrial viability (**$p < 0.0099$).

hence the IC_{50} concentration was not reached (Figure 8). The extrapolated values of cell viability (Table 1) indicated low

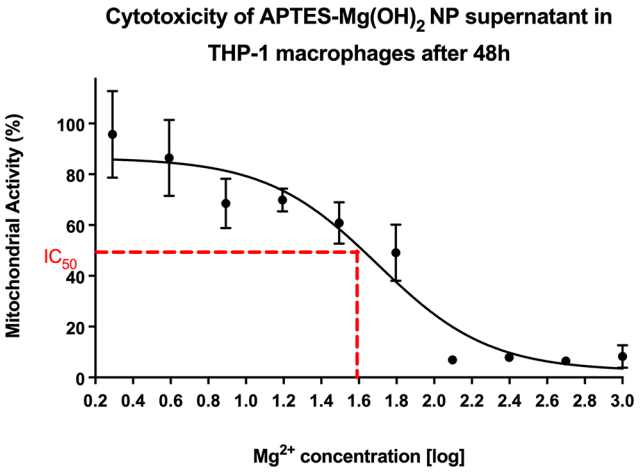

Figure 8. Mg^{2+} dosage in supernatant, which is 2500−19.5 μg/mL NPs concentration range does not reach the IC_{50} concentration indicated by the $MgCl_2$ standard curve. THP-1 macrophages were exposed to $MgCl_2$ (1−0.001 M, 10-fold serially diluted) for 48 h at 37 °C. IC_{50} concentration of 50 mmol/L was indicated in an MTT assay. The concentration of Mg^{2+} in NPs supernatants (6.50−0.30 mmol/L) did not reach the IC_{50} value hence it exhibited low adverse effects equivalent to ∼84% cell viability.

Table 1. Cell Viability of Supernatants Corresponding to Nanoparticle Concentration Range (2500−19.5 μg/mL) Extrapolated from the $MgCl_2$ Standard Curve and Shows No Cytotoxicity

APTES-$Mg(OH)_2$-NPs [μg/mL]	released Mg^{2+} [mmol/L]	released Mg^{2+} [log]	mitochondrial activity (%)
2500	6.50	0.81	82.5
1250	6.11	0.79	84
625	4.74	0.68	85
312.5	2.94	0.47	85

adverse effects of Mg^{2+} present in the NPs supernatant. Altogether, this suggests that the cell death observed in MTT assay upon high NP concentrations is not driven by $Mg(OH)_2$-NPs dissociation products in the culture medium.

3. DISCUSSION

In this study, we demonstrate low colloidal stability and strong aggregation of bare $Mg(OH)_2$-NPs, two characteristics that were strongly improved with NP surface functionalization. The limitations associated with bare NPs, can be attributed to the pH value of the reacting mixture during particle synthesis being near the isoelectric point of $Mg(OH)_2$-NPs in water (pH 12), which implies zero overall surface charge and low stability of the colloidal system. Moreover, the elevated pH with a large concentration of hydroxyl ions can generate tiny, not well-defined nuclei that tend to aggregate to lower their surface energy. When considering in vivo applications, such in situ aggregation would probably translate into rapid NP clearance in the liver, thus limiting the probability of reaching therapeutic targets upon NPs intravenous administration.[23] For this reason, surface functionalization was employed as a

https://doi.org/10.1021/acsomega.1c06515
ACS Omega 2022, 7, 17528−17537

strategy to improve colloidal stability and avoid persistent aggregation.

Functionalization of NPs with organosilane APTES resulted in higher particle colloidal stability, an observation in accordance following other studies.[24] Their dispersibility properties were further improved by including of protein, namely, FBS, in the cell culture media. This is in agreement with other reports, where FBS has been shown to improve the NP colloidal stability.[25] Additionally, the observed differences between different concentrations of added FBS also correlate with the fact that protein concentration plays a decisive role in determining the NP stabilization. Considering the high complexity of human physiological media and the known effect of particle surface opsonization upon blood or tissue contact,[26] increased stability upon in vitro FBS exposure indicates favorable outcomes when considering in vivo applications.

The zeta potential values of 36.8 ± 2.2 and 39.2 ± 1.4 mV for $Mg(OH)_2$-NPs without and with functionalization respectively, determines that the condition should be stable. That, however, is not observed in this case, as the nonfunctionalized NPs present little stability whereas the functionalized NPs remain dispersed for several hours. The increase in zeta potential is not considered big enough (it is only 2.4 mV) to explain this behavior; a difference of at least 10 mV is reported to be needed to show variation in stability of NPs.[27] Roland et al.[27] also reported that in some cases they did not find any correlation between stability and zeta potential; other factors might be more important in some cases, as appears to be the present situation, where electrostatic stabilization is not the main mechanism for stability.[28]

Altogether, surface functionalization of $Mg(OH)_2$-NPs and the presence of 10% FBS in cell culture media strongly improved the steric stability of NPs, hence the conditions and the relevance of the subsequent cytotoxic evaluations. Indeed, the evaluation of functionalized $Mg(OH)_2$-NPs in THP-1 macrophages resulted in an IC_{50} concentration of 1513 μg/mL, which was in line with other studies, where at 500[29] or 1000 μg/mL,[30] the IC_{50} in macrophages was not yet reached, respectively. While the cytotoxic evaluation did not exhibit a dose−response curve, the viability was strongly affected at 2500 μg/mL when an NPs crust on top of the cells was formed. This precipitate was observed in all the experiments, irrespective of the NPs type and colloidal characteristics, and was suggested as the main cause of NPs toxicity. Given that the precipitation was only detected above 625 μg/mL, this was hypothesized to be an inevitable concentration-dependent phenomenon, manifested upon reaching a certain concentration saturation point.

The dissolution of metal ions has previously been reported as one of the determinants for the toxic potential of metal-containing NPs.[31,32] Thus, aside from assessing the cytocompatibility of the NPs, we were also interested in differentiating the specific effects of Mg^{2+} concentration and alkaline pH on the THP-1 macrophage behavior. In line with the results obtained in cytotoxicity assays, high cytocompatibility of NP dissociation products has been observed. Namely, neither the alkaline media nor the respective Mg^{2+} levels of tested NP concentrations demonstrated adverse effects on THP-1 macrophage viability or morphology. Accordingly, NPs failed to exhibit an apparent dose−response effect, which would be present if their toxicity was transmitted through released OH^- or Mg^{2+} ions. Their cytotoxic properties were only demonstrated when the NPs crust was formed.

In concordance with our expectations, the Mg^{2+} release increased with $Mg(OH)_2$-NP concentration (Figure 5). Importantly, these increased Mg^{2+} ion levels in higher concentrations come from a low fraction of dissolved NPs, while low levels of released Mg^{2+}, observed in low NP concentrations, result from complete NP dissolution (Figure 6). This phenomenon could be attributed to the corresponding media pH. Indeed, the dissociation of $Mg(OH)_2$ is known to be heavily influenced by pH and temperature, with the physiological pH (7.2−8.2) promoting its dissociation.[33] The media pH of NP concentrations between 156.3 and 19.5 μg/mL (Figure 4) corresponds to this range, thus explaining higher NP dissociation in low concentrations. Indeed, another study confirmed full degradation, hence 100% dissociation, of $Mg(OH)_2$ NPs at 200 μg/mL.[33] Additionally the fact that $Mg(OH)_2$ precipitation counteracts its dissociation further explains low dissociation at high NP concentrations. Additionally, due to the result of functionalization of the NPs with the APTES shielding or because of an NPs aggregation which generate a thicker layer of material preventing the release of Mg^{2+}. Together with immediate media color change, an instant increase of Mg^{2+} levels and media pH without significant further changes over time indicates a rapid dissolution and high reactivity of $Mg(OH)_2$-NPs. Both media pH and Mg^{2+} release were found to be concentration-dependent phenomena. The proportion of dissolved NPs was concentration-dependent, with the lowest concentrations reaching almost complete dissolution, hence proposing their application in treating hypomagnesemia. Alternatively, most NPs remained in a solid-state at high concentrations, thus suggesting their potential as an NP delivery system. It has to be pointed out that a certain proportion of particles will always dissolve; hence their delivery efficiency will never reach 100%, and increased OH^- and Mg^{2+} levels will accompany every attempted application.

Lastly, the comparative analysis of toxic effects on different cell types showed important changes in the sensitivity to bare $Mg(OH)_2$-NPs. Irrespective of employing primary cells or cell lines, a higher sensitivity of endothelial cells (HUVECs, HPMECs) and macrophages (THP-1 cells) was observed when compared to fibroblasts (HDF, PK84) and ASCs.

Although the cellular uptake mechanisms of NPs were not dissected in this study, it is essential to consider this process in the cell-material interaction. The cytotoxic effect of the NPs is highly dependent on their nature, the concentration, and exposure time. It is expected that as Mg is an essential element for the body, it does not represent considerable side effects. Other features of the NPs, such as size, shape, surface chemistry, and surface energy, determine how cells and particles interact.[34] Generally, the uptake of the NPs involves processes as direct diffusion, micropinocytosis, endocytosis, phagocytosis, or adhesive interactions. Because the size of the $Mg(OH)_2$-NPs ranges in about 35−215 nm, the expected uptake pathways are endocytosis or diffusion for the smallest particles and via phagocytosis for the larger (including aggregated). However, more research is required for the $Mg(OH)_2$-NPs since their internalization may be highly affected by factors, such as protein adsorption and cell types.[34]

Together with the high cytocompatibility, these cellular responses discard the use of APTES-$Mg(OH)_2$-NPs as a toxic agent and instead suggest them as a potential drug delivery vehicle. By attaching targeting moieties to their surfaces, they

https://doi.org/10.1021/acsomega.1c06515
ACS Omega 2022, 7, 17528−17537

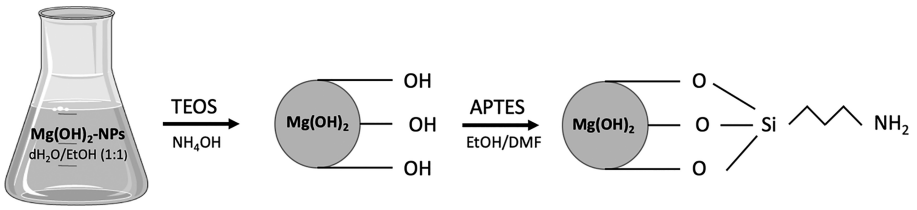

Figure 9. Functionalization process of the $Mg(OH)_2$-NPs with TEOS/APTES.

could deliver cargo (drugs or other therapeutic molecules) to targeted sites through ligand−receptor recognition, followed by receptor-mediated endocytosis and drug release inside the cell.

Since the pH values of tumor cells are lower than those of normal cells, Mg-NPs, which affect the pH of the environment, can be used as pH-responsive drug carriers to treat tumors. For example, Krishnamoorthy et al. showed that Mg-NPs could effectively kill cancer cells while healthy cells were less affected. The internalization of Mg-NPs can be used for different applications as intracellular trafficking (labeled with fluorescent labels) and as carriers to deliver specific biomolecules, such as drugs, genes, antimicrobial agents, and other molecules. The biofunctionalization of the NPs should consider aspects, such as delivering drug payloads, targeted cells, and the effect of the particles on the surrounding healthy tissues and organs. The main advantages of using Mg-NPs as drug delivery systems rely on the facile and low-cost synthesis, the high surface area available, and its high stability.[35,36]

4. CONCLUSIONS

In summary, the characterization of bare $Mg(OH)_2$-NPs revealed high colloidal instability with increased sedimentation rates. Surface functionalization of $Mg(OH)_2$-NPs with an organosilane (APTES) improved these physicochemical characteristics. However, a time-dependent decline in colloidal stability could still be observed. Mg-based NPs, and their dissociation products, namely, released OH^- and Mg^{2+} ions, exhibited low toxic properties toward the investigated in vitro models. Among the investigated cell types, HDF, ASCs, and PK84 fibroblasts proved to be the most resistant, while HUVECs, HPMECs, and THP-1 cells were the most susceptible to toxic effects. To conclude, the demonstrated high $Mg(OH)_2$-NPs cytocompatibility demonstrates their potential as drug delivery vehicles.

However, their physicochemical characteristics need to be further improved and more thoroughly investigated. Additionally, it is crucial to study the pathways of cellular and intracellular behaviors of $Mg(OH)_2$-NPs to understand their biological effects better and optimize their clinical applications.

5. MATERIALS AND METHODS

5.1. Generation of $Mg(OH)_2$-NPs. $Mg(OH)_2$-NPs were prepared by the coprecipitation method.[22] Briefly, 1 M NaOH aqueous solution (Merck Millipore, Darmstadt, Germany, ≥99%) was added dropwise into an aqueous solution of 1 M $MgCl_2$−$6H_2O$ (PanReac AppliChem, Chicago IL, US) to a glass beaker (500 mL), while gently stirring for 10 min. The obtained mixture was left undisturbed to sediment at room temperature (RT) for an additional 48 h. The chemical reaction involved in the formation of NPs was as follows:

$$MgCl_2(aq) + 2NaOH(aq) \rightarrow Mg(OH)_2(s) \downarrow + 2NaCl(aq)$$

The precipitate was collected by centrifugation (300*g*, 5 min) and washed four times with deionized water (dH_2O) and twice with 99.9% ethanol (EtOH) (Merck, New Jersey, US). Initially, the as-prepared $Mg(OH)_2$-NPs were dried in a vacuum at 60 °C. Alternatively, when $Mg(OH)_2$-NPs were synthesized de novo, they were kept in 99.9% EtOH (Merck, New Jersey, US) at RT and resuspended in ethanol to increase the stability of the particles and enhance particle dispersion and homogeneity.

5.2. Characterization of the NPs. The average size and concentration (particles per milliliter) of the NPs were determined using a NanoSight LM10 (Malvern Panalytical, UK) with Nanoparticle Tracking Analysis (NTA) software. In principle: particles were prepared in a 2% w/v suspension using PBS (Invitrogen, Chicago IL, US). After analysis by NTA, the total volume of particles was calculated using the average size and the total number of particles in the stock solution. Concentration in the stock solution (μg/mL) was ultimately determined. The results were expressed in the mean sizes and standard error of at least three individual measurements. The morphology of the NPs was assessed by transmission electron microscopy (TEM)(FEI Tecnai G2 F20 S-TWIN). For measuring the zeta potential of the NPs, it was employed a NanoPlus HD, Particulate Systems of micromeritics. The samples were taken from a 1:10 dilution of the NPs suspension, both without functionalization and functionalized. The assays were carried out by triplicate for each sample and the average values were employed for the analysis.

5.3. Functionalization of $Mg(OH)_2$-NPs. Because of persistent aggregation, $Mg(OH)_2$-NPs were prepared as described above and subjected to surface functionalization with two aminosilanes: tetraethoxysilane (TEOS, Sigma-Aldrich, 98%) and 3-aminopropyltriethoxysilane (APTES, Sigma-Aldrich, St. Louis, USA, 99%). A solution of 0.4 g of NPs dispersed in 60 mL of dH_2O/EtOH (1:1) solution at 40 °C and constant stirring were used. Further, 1.2 mL of TEOS was dropwise added at the time that the temperature was increasing to 50 °C. After 6 h, 1.2 mL of NH_4OH_2 was added as a precursor of the salinization reaction. The mixture remained under constant stirring for 24 h. NPs were washed several times with ethanol by centrifugation (300*g*) to eliminate possible excesses of the reaction. Then, the NPs were dispersed in 60 mL of *N*,*N*-dimethylformamide (DMF, Merck Millipore) at a temperature of 60 °C and stirring at 200*g*, where 1.2 mL of APTES was added during constant stirring for 24 h. Finally, the NPs were washed several times with ethanol at 300*g* for 5 min (see Figure 9).

To determine their dispersible property, bare and differently functionalized $Mg(OH)_2$ NPs were incubated and macro-

https://doi.org/10.1021/acsomega.1c06515
ACS Omega 2022, 7, 17528−17537

scopically monitored in ethanol, distilled H_2O, culture mediums RPMI-1640 (Lonza, Basel, Switzerland), DMEM (Lonza, Basel, Switzerland), DMEM with 3% fetal bovine serum (FBS) (Lonza, Basel, Switzerland) and DMEM with 10% FBS at RT for 48 h. Dispersion of NPs described as the qualitative turbidity of the solution was studied after 1, 24, and 48 h in solutions as dH_2O, cell culture medium, and EtOH.

5.4. Analysis of the Dissolution of APTES-$Mg(OH)_2$-NPs in Culture Media. The dissolution of APTES-$Mg(OH)_2$-NPs and their effect on media pH was analyzed in the conditions mimicking the toxicity and uptake assays. For the former, NPs (0−2.500 μg/mL) were incubated under standard cell culture conditions for 48h, centrifuged (1000*g*, 5 min), and the media were collected to determine Mg^{2+} concentration using inductively coupled plasma mass spectrometry (ICP-MS) (Varian 820 ms, Palo Alto, CA, US). Following the same protocol, Mg^{2+} release was measured after 1, 3, 6, 12, 24, 48, 72, and 96 h incubation at the selected concentration of 300 μg/mL.

5.5. Biological Evaluation of the $Mg(OH)_2$-NPs. *5.5.1. Cell Culture and Exposure Conditions.* Initial screening to study the toxicity effect of the $Mg(OH)_2$-NPs was performed using the following cells: human dermal fibroblasts (HDF), human umbilical vein endothelial cells (HUVEC, Lonza, MD, USA), human pulmonary microvascular endothelial cell line (HPMEC), human skin fibroblast cell line (PK84), monocytic cell line (THP-1) (TIB-202, ATCC, USA), and primary adipose tissue-derived stromal/stem cells (ASC). ASCs were obtained from adipose tissue from human subcutaneous tissue acquired through liposuction from three different donors. HDF, PK84, and ASCs were cultured in high glucose DMEM with 10% FBS. HUVEC and HPMEC were seeded on substrate precoated with 1% gelatin and cultured in an endothelial cell medium (ECM) consisting of RPMI-1640 (Biowhittaker, Verviers, Belgium), 10% fetal bovine serum (FBS) (Thermo Scientific, Hemel Hempstead, UK), 0.06 mg/mL of homemade bovine brain-derived extract (endothelial cell growth factor, ECGF), 0.1 mg/mL heparin (Leo Pharma, Netherlands), 1% penicillin/streptomycin (Gibco, Invitrogen, Carlsbad, CA), and 2 mM L-glutamine (Lonza, Biowhittaker, Verviers, Belgium). Suspensions of THP-1 cells were cultured in an RPMI medium containing 25 mM HEPES (Lonza), and supplemented with 10% of FBS. All cell cultures were provided with 1% v/v penicillin−streptomycin and 2 mM L-glutamine (both Lonza). All the experiments were performed when the confluence was reached (HDF, HUVEC, HPMEC, PK84, and ASC), except for THP-1 cells that were passaged the same day if used as monocytes or were differentiated into macrophages by adding 10 ng/mL PMA for 72 h before the experiment.

5.5.2. $Mg(OH)_2$-NPs Preparation for Toxicity Assays. A stock solution of 2.500 μg/mL $Mg(OH)_2$-NPs was kept in 99,9% EtOH, ultrasonicated immediately prior to use (BANDELIN ElectronicGmbH & Co. KG, Berlin, Germany) for 5 min and dried at 55 °C. Before cell exposure, a stock solution was prepared in the appropriate cell culture medium corresponding to the adequate cell group and ultrasonicated directly for 5 min. Upon the generation of APTES-$Mg(OH)_2$-NPs, the appropriate NP solution was prepared by directly resuspending final functionalized NPs in medium with 10% ethanol or only medium, respectively, followed by 30 min in a conventional ultrasonic bath (BANDELIN ElectronicGmbH & Co. KG, Berlin, Germany) with 35 kHz operating frequency and a maximum power of 480 W.

5.5.3. Toxicity of $Mg(OH)_2$-NPs in Different Cell Lines. Cytotoxic activities were determined using a 3-(4,5-dimethylthiazol-2-yl)-2,5-diphenyltetrazolium bromide (MTT) assay. According to its growth curve, cells were seeded in 96 wells culture plates at initial densities of 25 000 cells/well (PK84), 50 000 cells/well (HDF, HUVEC, HPMEC, and ASCs), or 30 000 cells/well (THP-1), and incubated at 37 °C in a humidified 5% CO_2 atmosphere. When confluence or differentiated state was reached, the medium was replaced with 100 μL of respective nanoparticle concentration. 2-Fold serial dilutions were performed to obtain $Mg(OH)_2$-NPs suspensions ranging from 2.500 to 19.5 μg/mL. In all assays, cells free of NPs served as a negative control. Respective NP dilution in acellular conditions was included to correct for their background effect. After 48 h incubation, 20 μL of 5 mg/mL MTT (Sigma-Aldrich) in PBS was added into each well and incubated for 3 h at 37 °C in the incubator. Then, the supernatant was carefully discarded without disturbing the formed crystals, and 100 μL of DMSO (Merck Millipore) was added to dissolve formazan crystals. For the THP-1 suspension cultures, culture plates were centrifuged (300*g*, 5 min) to pellet the cells on the bottom. After mixing, optical densities at 570 and 650 nm were read with a Benchmark plus (Bio-Rad) plate reader. MTT assay is used to measure cellular metabolic activity by converting of NAD(P)H-dependent oxidoreductase enzymes, which reduce the MTT to formazan. This reaction is used to indicate cell viability, proliferation, and cytotoxicity. In this way, the mitochondrial activity was calculated as the mean of optical density obtained for each condition and normalized to the negative control.

5.5.4. Effect of Metal Ion Release in Cell Activity. To assess the impact of potentially shed metal ions, a calibration curve (1−0.001M, 10-fold serially diluted) of $MgCl_2{-}6H_2O$ was generated in respective cell culture media. Its toxic effect on THP-1 macrophages was determined by MTT conversion. The media pH was monitored in all the concentrations after 5 min, 15 min, 1 h, 3 h, 6 h, 12 h, 24 h, and 48 h of incubation. To further delineate its cytotoxic effect, five nanoparticle concentrations (2.500, 1.250, 312, 39, 19 μg/mL) were incubated under standard culture conditions for 48 h. Following centrifugation (1000*g*, 5 min), the toxicity of the supernatant with adjusted (pH 7.5) or nonadjusted pH was investigated in an MTT assay in THP-1 macrophages. Additionally, a cytotoxicity test was carried out with the APTES-$Mg(OH)_2$-NPs using THP-1 cells. Results from cells without any NP treatment were used as control. All the results were expressed in terms of the percentage of mitochondrial activity and were normalized to the control.

5.5.5. Statistical Analysis. All cytotoxicity experiments were performed in triplicate and repeated at least twice. All data are represented as means ± standard deviation and were analyzed by two-way ANOVA. Where possible, toxicity values were calculated by the logarithmic transformation of *x*-values and plotted using GraphPad Prism software, version 7.03 (GraphPad Software, San Diego, California, USA).

■ ASSOCIATED CONTENT

Supporting Information

The Supporting Information is available free of charge at https://pubs.acs.org/doi/10.1021/acsomega.1c06515.

Immunofluorescent staining materials and methods and fluorescence images, dispersion of APTES-coated NPs in

https://doi.org/10.1021/acsomega.1c06515
ACS Omega 2022, 7, 17528−17537

different solutions, and images of THP-1 exposed to $Mg(OH)_2$-NPs with alkaline and neutral pH (PDF)

AUTHOR INFORMATION

Corresponding Authors

Mónica Echeverry-Rendón − *IMDEA Materials Institute, Getafe, Madrid 28906, Spain; University of Groningenn, University Medical Center Groningen, Department of Pathology and Medical Biology, NL-9713 GZ Groningen, The Netherlands; Centro de Investigación, Innovación y Desarrollo de Materiales (CIDEMAT), Facultad de Ingeniería, Universidad de Antioquia, Medellín 050010, Colombia;* orcid.org/0000-0002-7452-0987; Email: monica.echeverry@imdea.org

Martin C. Harmsen − *University of Groningenn, University Medical Center Groningen, Department of Pathology and Medical Biology, NL-9713 GZ Groningen, The Netherlands;* Email: m.c.harmsen@umcg.nl

Authors

Brina Stančič − *University of Groningenn, University Medical Center Groningen, Department of Pathology and Medical Biology, NL-9713 GZ Groningen, The Netherlands; Department of Molecular Biology, Universidad Autónoma de Madrid, and Department of Molecular Neuropathology, Center of Molecular Biology Severo Ochoa (UAM-CSIC), 28049 Madrid, Spain*

Kirsten Muizer − *University of Groningenn, University Medical Center Groningen, Department of Pathology and Medical Biology, NL-9713 GZ Groningen, The Netherlands*

Valentina Duque − *Centro de Investigación, Innovación y Desarrollo de Materiales (CIDEMAT), Facultad de Ingeniería, Universidad de Antioquia, Medellín 050010, Colombia*

Deanne Jennei Calderon − *Centro de Investigación, Innovación y Desarrollo de Materiales (CIDEMAT), Facultad de Ingeniería, Universidad de Antioquia, Medellín 050010, Colombia*

Felix Echeverria − *Centro de Investigación, Innovación y Desarrollo de Materiales (CIDEMAT), Facultad de Ingeniería, Universidad de Antioquia, Medellín 050010, Colombia*

Complete contact information is available at: https://pubs.acs.org/10.1021/acsomega.1c06515

Notes

The authors declare no competing financial interest.

ACKNOWLEDGMENTS

M.E.R. acknowledges the support of the Spanish Ministry of Science and Innovation through the Juan de la Cierva-Formation fellowship FJC2019-039925-I

REFERENCES

(1) Krishnamoorthy, K.; Moon, J. Y.; Hyun, H. B.; Cho, S. K.; Kim, S.-J. Mechanistic investigation on the toxicity of MgO nanoparticles toward cancer cells. *J. Mater. Chem.* **2012**, *22* (47), 24610−7.

(2) Bahadar, H.; Maqbool, F.; Niaz, K.; Abdollahi, M. Toxicity of nanoparticles and an overview of current experimental models. *Iran. Biomed. J.* **2016**, *20* (1), 1−11.

(3) Yazdani, S.; Bansal, R.; Prakash, J. Drug targeting to myofibroblasts: Implications for fibrosis and cancer. *Adv. Drug Deliv Rev.* **2017**, *121*, 101−116.

(4) Khanna, P.; Ong, C.; Bay, B. H.; Baeg, G. H. Nanotoxicity: An interplay of oxidative stress, inflammation and cell death. *Nanomaterials* **2015**, *5* (3), 1163−1180.

(5) Mahmoud, A.; Ezgi, Ö; Merve, A.; Özhan, G. In Vitro Toxicological Assessment of Magnesium Oxide Nanoparticle Exposure in Several Mammalian Cell Types. *Int. J. Toxicol* **2016**, *35* (4), 429−37.

(6) Dong, C.; Song, D.; Cairney, J.; Maddan, O. L.; He, G.; Deng, Y. Antibacterial study of Mg(OH)2 nanoplatelets. *Mater. Res. Bull.* **2011**, *46* (4), 576−82.

(7) Wetteland, C. L.; Nguyen, N. Y. T.; Liu, H. Concentration-dependent behaviors of bone marrow derived mesenchymal stem cells and infectious bacteria toward magnesium oxide nanoparticles. *Acta Biomater* **2016**, *35*, 341−56.

(8) Sawai, J.; Kojima, H.; Igarashi, H.; Hashimoto, A.; Shoji, S.; Sawaki, T.; Hakoda, A.; Kawada, E.; Kokugan, T.; Shimizu, M. Antibacterial characteristics of magnesium oxide powder. *World J. Microbiol. Biotechnol.* **2000**, *16* (2), 187−94.

(9) He, Y.; Ingudam, S.; Reed, S.; Gehring, A.; Strobaugh, T. P.; Irwin, P. Study on the mechanism of antibacterial action of magnesium oxide nanoparticles against foodborne pathogens. *J. Nanobiotechnol* **2016**, *14* (1), 54.

(10) Nygren, H.; Chaudhry, M.; Gustafsson, S.; Kjeller, G.; Malmberg, P.; Johansson, K.-E. Increase of Compact Bone Thickness in Rat Tibia after Implanting MgO into the Bone Marrow Cavity. *J. Funct Biomater* **2014**, *5* (3), 158−66.

(11) Hickey, D. J.; Ercan, B.; Sun, L.; Webster, T. J. Adding MgO nanoparticles to hydroxyapatite-PLLA nanocomposites for improved bone tissue engineering applications. *Acta Biomater* **2015**, *14*, 175−84.

(12) Suryavanshi, A.; Khanna, K.; Sindhu, K. R.; Bellare, J.; Srivastava, R. Magnesium oxide nanoparticle-loaded polycaprolactone composite electrospun fiber scaffolds for bone−soft tissue engineering applications: in-vitro and in-vivo evaluation. *Biomed Mater.* **2017**, *12* (5), 055011.

(13) Kumaran, R. S.; Choi, Y. K.; Singh, V.; Song, H. J.; Song, K. G.; Kim, K. J.; Kim, H. J. In Vitro cytotoxic evaluation of MgO nanoparticles and their effect on the expression of ROS genes. *Int. J. Mol. Sci.* **2015**, *16* (4), 7551−64.

(14) Ivask, A.; Titma, T.; Visnapuu, M.; Vija, H.; Kakinen, A.; Sihtmae, M.; Pokhrel, S.; Madler, L.; Heinlaan, M.; Kisand, V.; Shimmo, R.; Kahru, A. Toxicity of 11 metal oxide nanoparticles to three mammalian cell types in vitro. *Curr. Top Med. Chem.* **2015**, *15* (18), 1914−29.

(15) Ge, S.; Wang, G.; Shen, Y.; Zhang, Q.; Jia, D.; Wang, H.; Dong, Q.; Yin, T. Cytotoxic effects of MgO nanoparticles on human umbilical vein endothelial cells in vitro. *IET Nanobiotechnology* **2011**, *5* (2), 36−40.

(16) Gelli, K.; Porika, M.; Anreddy, R. N. R. Assessment of pulmonary toxicity of MgO nanoparticles in rats. *Environ. Toxicol* **2015**, *30* (3), 308−14.

(17) Meng, N.; Han, L.; Pan, X. H.; Su, L.; Jiang, Z.; Lin, Z.; Zhao, J.; Zhang, S. L.; Zhang, Y.; Zhao, B. X.; Miao, J. Y. Nano-Mg(OH)2-induced proliferation inhibition and dysfunction of human umbilical vein vascular endothelial cells through caveolin-1-mediated endocytosis. *Cell Biol. Toxicol* **2015**, *31* (1), 15−27.

(18) Pan, Z.; Lee, W.; Slutsky, L.; Clark, R. A. F.; Pernodet, N.; Rafailovich, M. H. Adverse effects of titanium dioxide nanoparticles on human dermal fibroblasts and how to protect cells. *Small* **2009**, *5* (4), 511−20.

(19) Zhang, C.; Ni, D.; Liu, Y.; Yao, H.; Bu, W.; Shi, J. Magnesium silicide nanoparticles as a deoxygenation agent for cancer starvation therapy. *Nat. Nanotechnol* **2017**, *12* (4), 378−86.

(20) Sajid, M.; Ilyas, M.; Basheer, C.; Tariq, M.; Daud, M.; Baig, N.; Shehzad, F. Impact of nanoparticles on human and environment: review of toxicity factors, exposures, control strategies, and future prospects. *Environ. Sci. Pollut Res.* **2015**, *22* (6), 4122−43.

(21) Ajdary, M.; Moosavi, M. A.; Rahmati, M.; Falahati, M.; Mahboubi, M.; Mandegary, A.; Jangjoo, S.; Mohammadinejad, R.;

https://doi.org/10.1021/acsomega.1c06515
ACS Omega 2022, 7, 17528−17537

Varma, R. S. Health Concerns of Various Nanoparticles: A Review of Their in Vitro and in Vivo Toxicity. *Nanomater* **2018**, *8* (9), 634.
(22) Calderón, D. J.; DeAlba-Montero, I.; Ruiz, F.; Echeverría, F. Effect of synthesis variables on the characteristics of magnesium hydroxide nanoparticles and evaluation of the fluorescence of functionalised Mg(OH)2 nanoparticles. *Adv. Nat. Sci. Nanosci Nanotechnol* **2020**, *11* (2), 025008.
(23) Lin, Y.-S.; Hurley, K. R.; Haynes, C. L. Critical Considerations in the Biomedical Use of Mesoporous Silica Nanoparticles. *J. Phys. Chem. Lett.* **2012**, *3* (3), 364−74.
(24) Graf, C.; Gao, Q.; Schütz, I.; Noufele, C. N.; Ruan, W.; Posselt, U.; Korotianskiy, E.; Nordmeyer, D.; Rancan, F.; Hadam, S.; Vogt, A.; Lademann, J.; et al. Surface functionalization of silica nanoparticles supports colloidal stability in physiological media and facilitates internalization in cells. *Langmuir* **2012**, *28* (20), 7598−7613.
(25) Moore, T. L.; Rodriguez-Lorenzo, L.; Hirsch, V.; Balog, S.; Urban, D.; Jud, C.; Rothen-Rutishauser, B.; Lattuada, M.; Petri-Fink, A. Nanoparticle colloidal stability in cell culture media and impact on cellular interactions. *Chem. Soc. Rev.* **2015**, *44* (17), 6287−6305.
(26) Gustafson, H. H.; Holt-Casper, D.; Grainger, D. W.; Ghandehari, H. Nanoparticle Uptake: The Phagocyte Problem. *Nano Today* **2015**, *10* (4), 487−510.
(27) Roland, I.; Piel, G.; Delattre, L.; Evrard, B. Systematic characterization of oil-in-water emulsions for formulation design. *Int. J. Pharm.* **2003**, *263*, 85−94.
(28) Kulkarni, N. S.; Ranpise, N. S.; Rathore, D. S.; Dhole, S. N. Characterization of Self-Microemulsifying Dosage Form: Special Emphasis on Zeta Potential Measurement. *International Journal of Pharmaceutical & Biological Archive* **2019**, *10* (3), 172−179.
(29) Roth, I.; Schumacher, S.; Basler, T.; Baumert, K.; Seitz, J.-M.; Evertz, F.; Müller, P. P.; Bäumer, W.; Kietzmann, M. Magnesium corrosion particles do not interfere with the immune function of primary human and murine macrophages. *Prog. Biomater.* **2015**, *4* (1), 21−30.
(30) Alvarez, F.; Lozano Puerto, R. M.; Pérez-Maceda, B.; Grillo, C. A.; Fernández Lorenzo de Mele, M. Time-Lapse Evaluation of Interactions Between Biodegradable Mg Particles and Cells. *Microsc Microanal.* **2016**, *22* (1), 1−12.
(31) Brunner, T. J.; Wick, P.; Manser, P.; Spohn, P.; Grass, R. N.; Limbach, L. K.; Bruinink, A.; Stark, W. J. In vitro cytotoxicity of oxide nanoparticles: comparison to asbestos, silica, and the effect of particle solubility. *Environ. Sci. Technol.* **2006**, *40* (14), 4374−81.
(32) Horie, M.; Fujita, K.; Kato, H.; Endoh, S.; Nishio, K.; Komaba, L. K.; Nakamura, A.; Miyauchi, A.; Kinugasa, S.; Hagihara, Y.; Niki, E.; Yoshida, Y.; Iwahashi, H. Association of the physical and chemical properties and the cytotoxicity of metal oxide nanoparticles: metal ion release, adsorption ability and specific surface area. *Metallomics* **2012**, *4* (4), 350−60.
(33) Wetteland, C. L.; de Jesus Sanchez, J.; Silken, C. A.; Nguyen, N-YT; Mahmood, O.; Liu, H. Dissociation of magnesium oxide and magnesium hydroxide nanoparticles in physiologically relevant fluids. *J. Nanoparticle Res.* **2018**, *20* (8), 215.
(34) Wu, M.; Guo, H.; Liu, L.; Liu, Y.; Xie, L. Size-dependent cellular uptake and localization profiles of silver nanoparticles. *Int. J. Nanomedicine.* **2019**, *14*, 4247−4259.
(35) Karlsson, O. J.; Schade, B. E. H. Particle Analysis: Particle Size, Particle Shape and Structure and Surface Characterisation. *Chemistry and Technology of Emulsion Polymerisation* **2007**, 186−225.
(36) Chen, Y.; Renner, P.; Liang, H. Dispersion of Nanoparticles in Lubricating Oil: A Critical Review. *Lubr* **2019**, *7* (1), 7.

https://doi.org/10.1021/acsomega.1c06515
ACS Omega 2022, 7, 17528−17537